Supporting Information

Feedback inhibition of DszC, a crucial enzyme for crude oil biodessulfurization

*Rui P. P. Neves,‡ Bruno M. V. Araújo,‡ Maria J. Ramos, Pedro A. Fernandes**

LAQV, REQUIMTE, Departamento de Química e Bioquímica, Faculdade de Ciências, Universidade do Porto, Rua do Campo Alegre, s/n, 4169-007 Porto, Portugal

*E-mail for P.A.F.: pafernan@fc.up.pt.

INDEX

Structural analysis of DszC

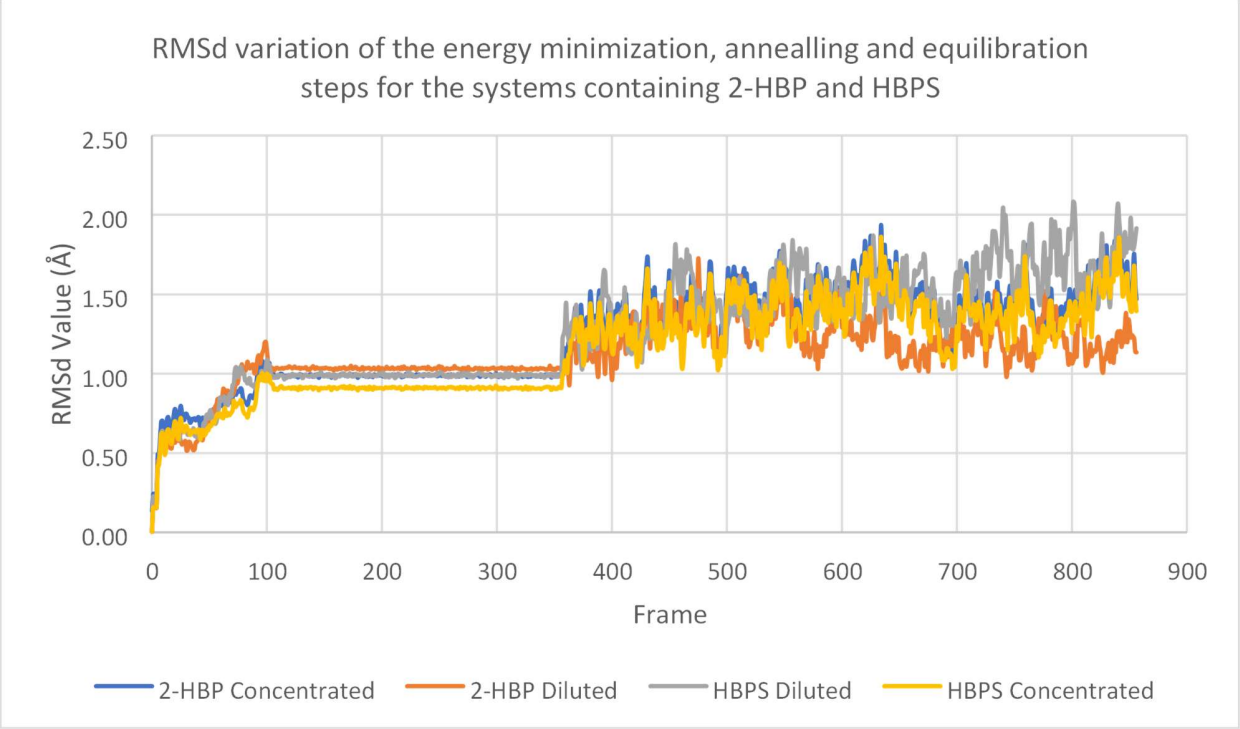

Figure S1. Graphical representation of the RMSd of the protein backbone over time. In the xx axis it is represented the number of frames and on the yy axis the RMSd value. The first 5 frames correspond to the initial structure and the four steps of the energy minimization protocol. Frames 5 to 110 correspond to the annealing protocol. Frames 110 to 383, demonstrate the enzyme behavior during the restrained portion of the equilibration phase for 10ns. The remaining corresponds to the RMSd value of the backbone during the unrestrained equilibration of 10ns.

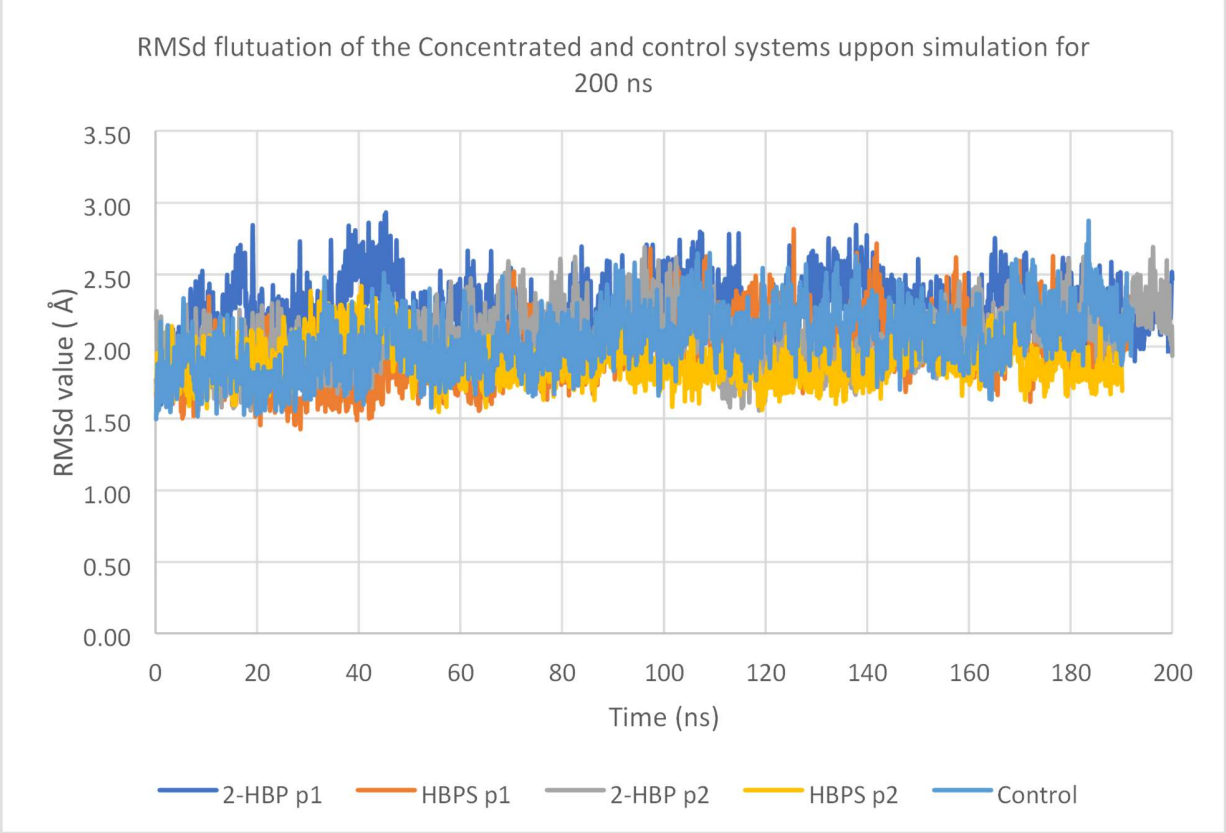

Figure S2. Graphical representation of the backbone RMSd fluctuation of the concentrated and control systems upon 200 ns simulation. In the legend, "p1" and "p2" refer to systems submitted to protocol 1 and protocol 2, respectively.

Interaction of 2-HBP and HBPS ligands with DszC throughout every 200 ns MD simulation

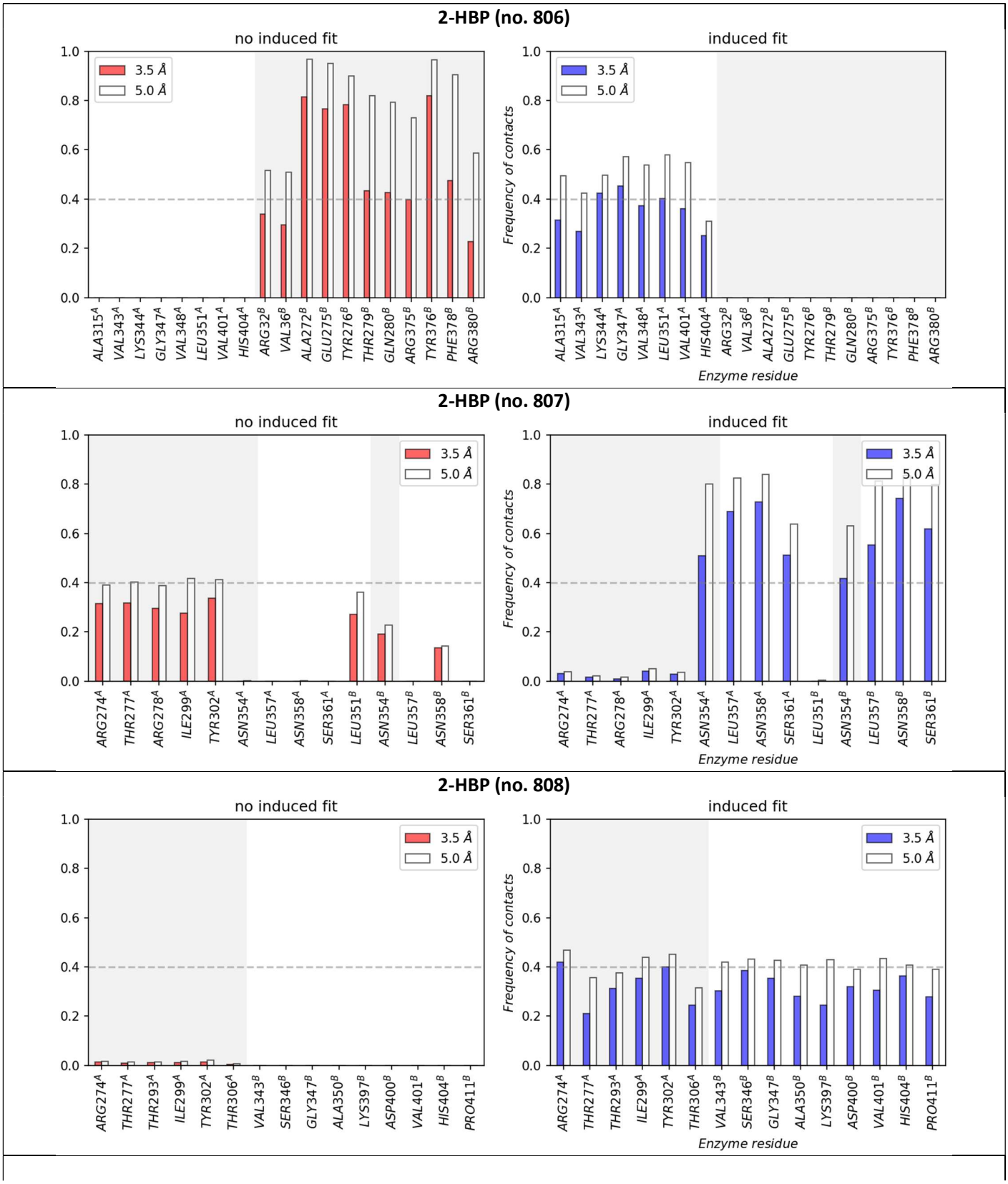

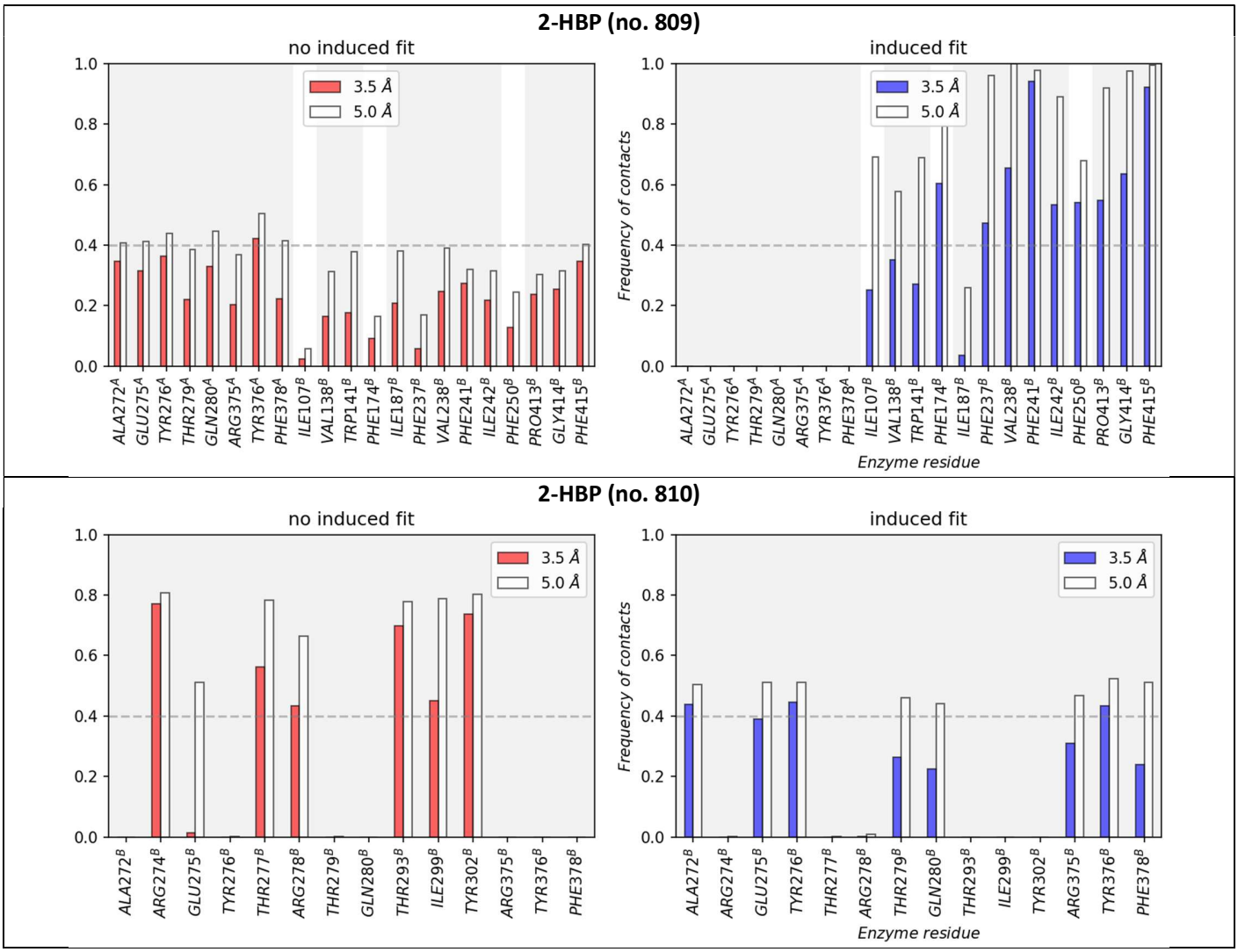

Figure S3. Bar plot of the frequency of contacts between different 2-HBP ligands and the DszC residues in the 200 ns MD simulations including five 2-HBP molecules.

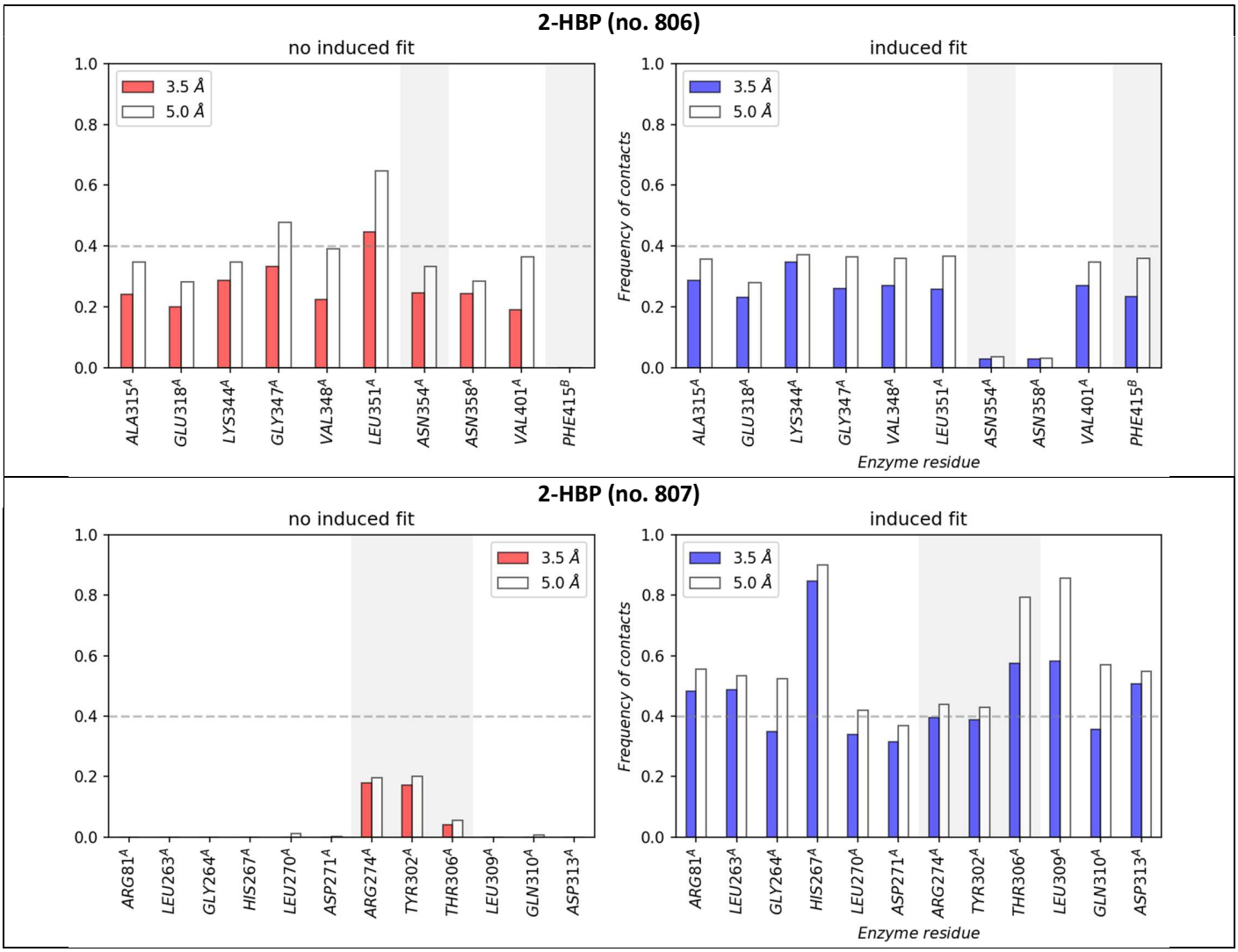

Figure S4. Bar plot of the frequency of contacts between different 2-HBP ligands and the DszC residues in the 200 ns MD simulations including two 2-HBP molecules

HBPS (no. 806)

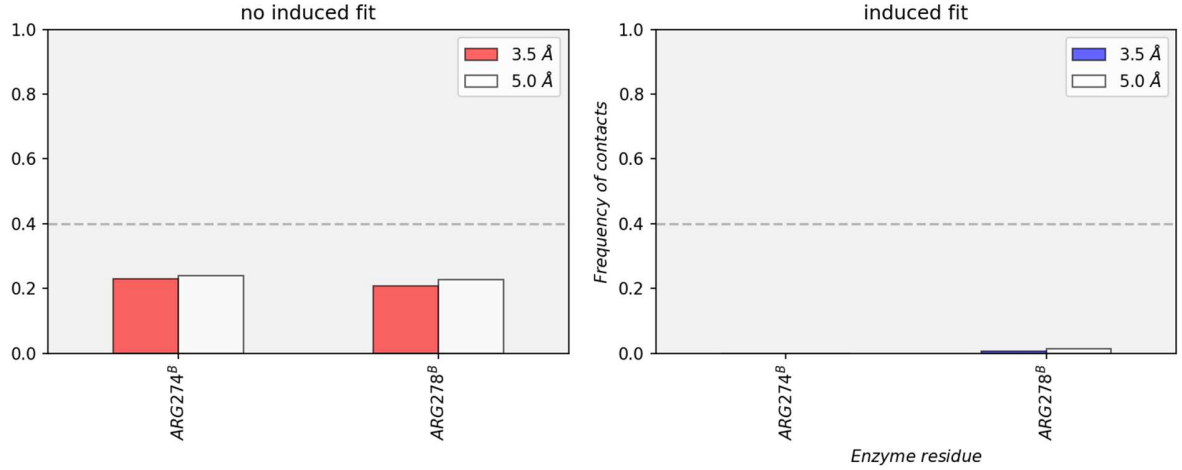

HBPS (no. 807)

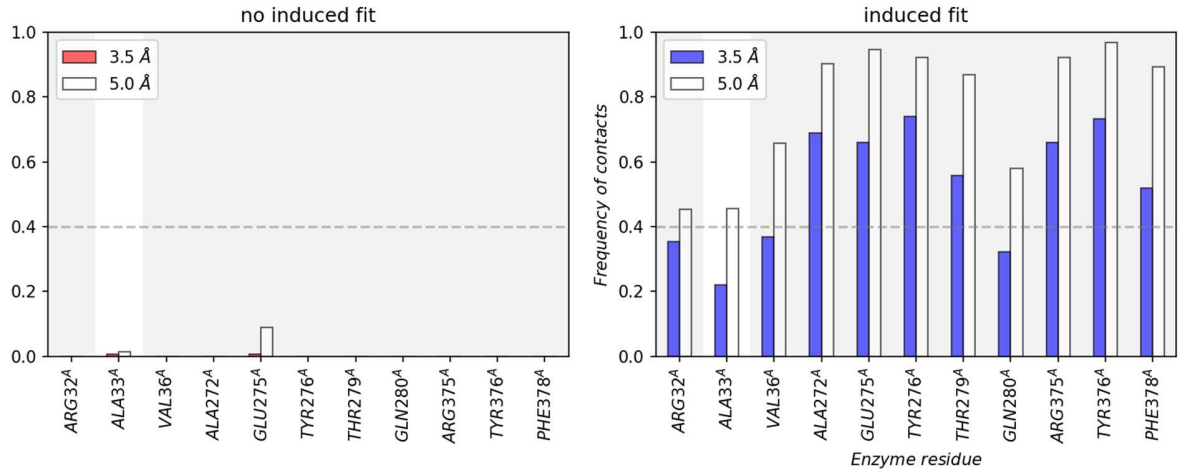

HBPS (no. 808)

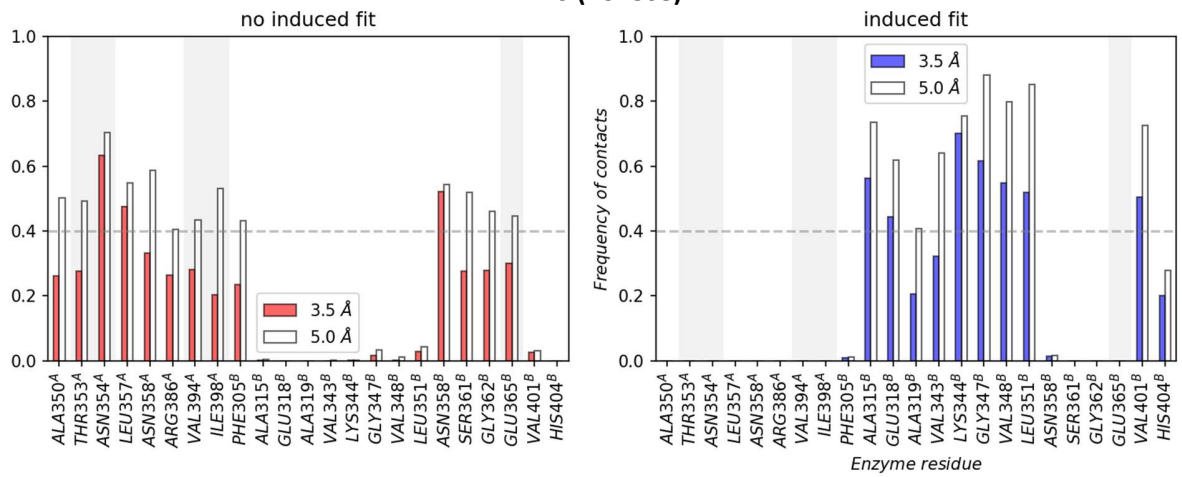

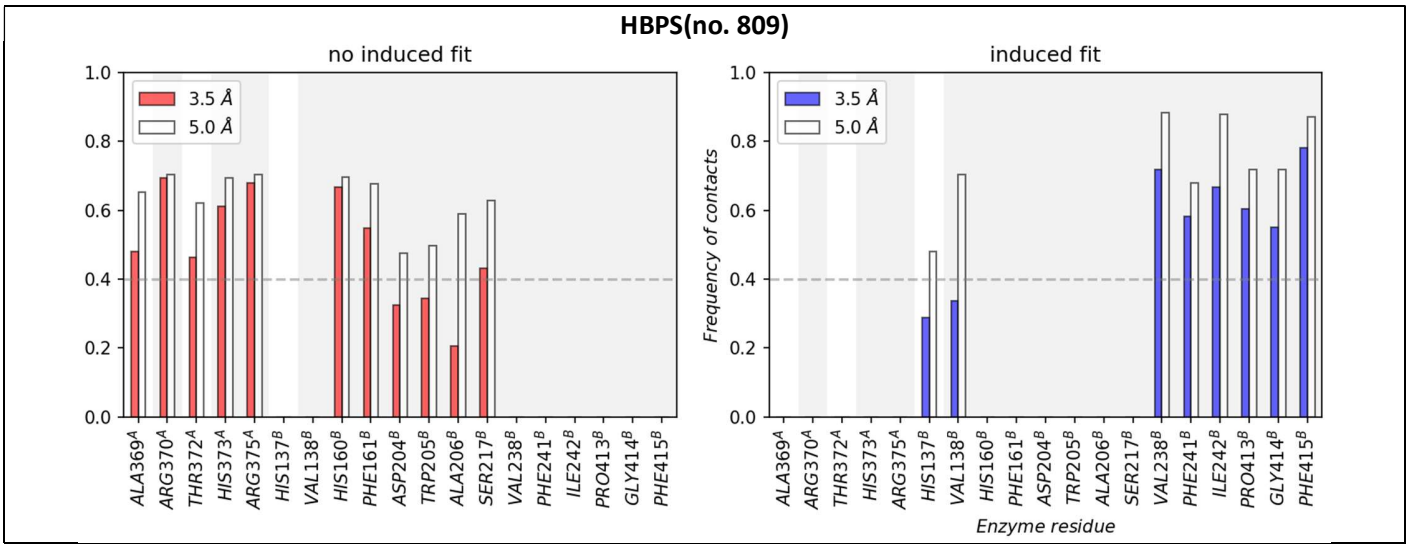

Figure S5. Bar plot of the frequency of contacts between different 2-HBP ligands and the DszC residues in the 200 ns MD simulations including four HBPS molecules.

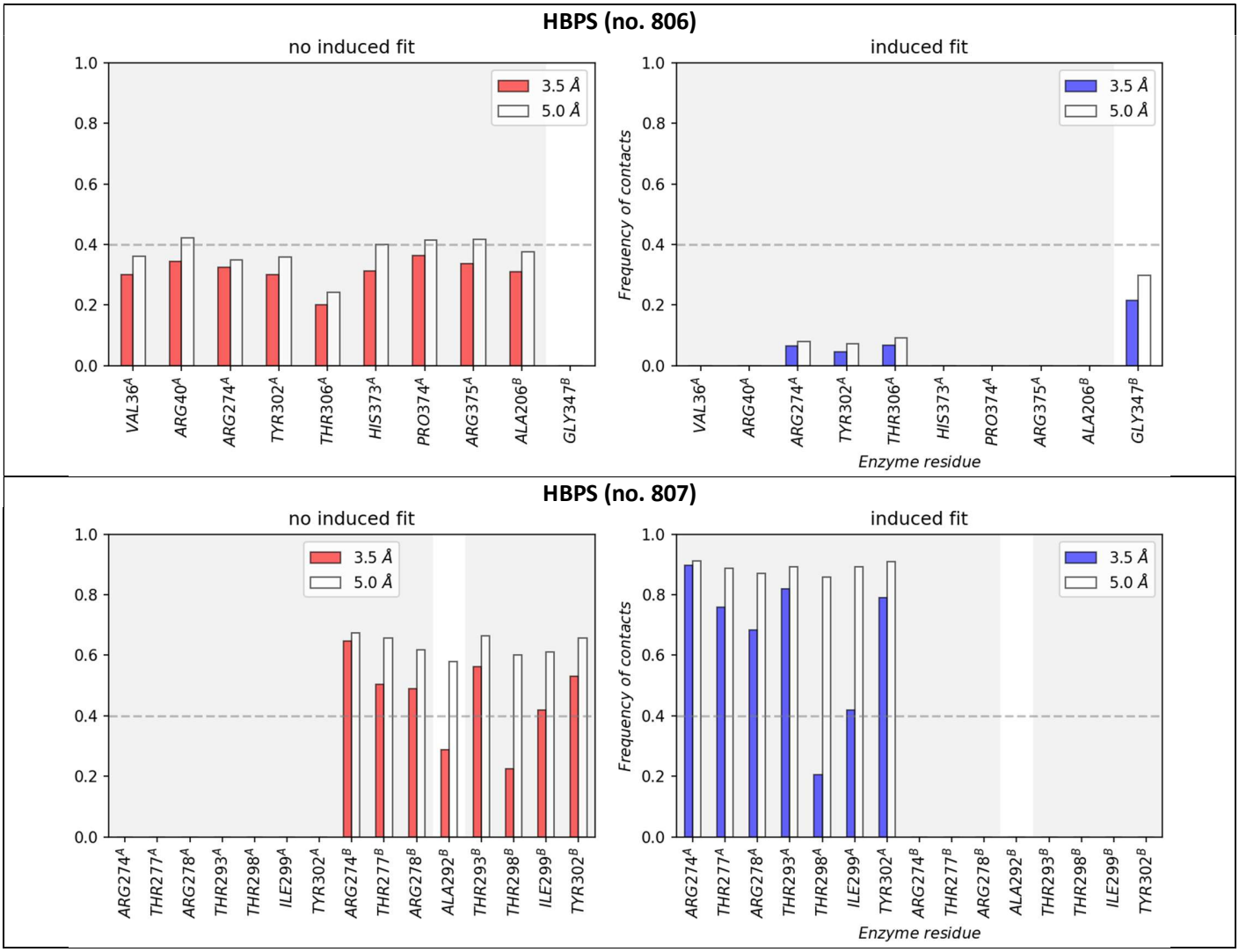

Figure S6. Bar plot of the frequency of contacts between different 2-HBP ligands and the DszC residues in the 200 ns MD simulations including two HBPS molecules

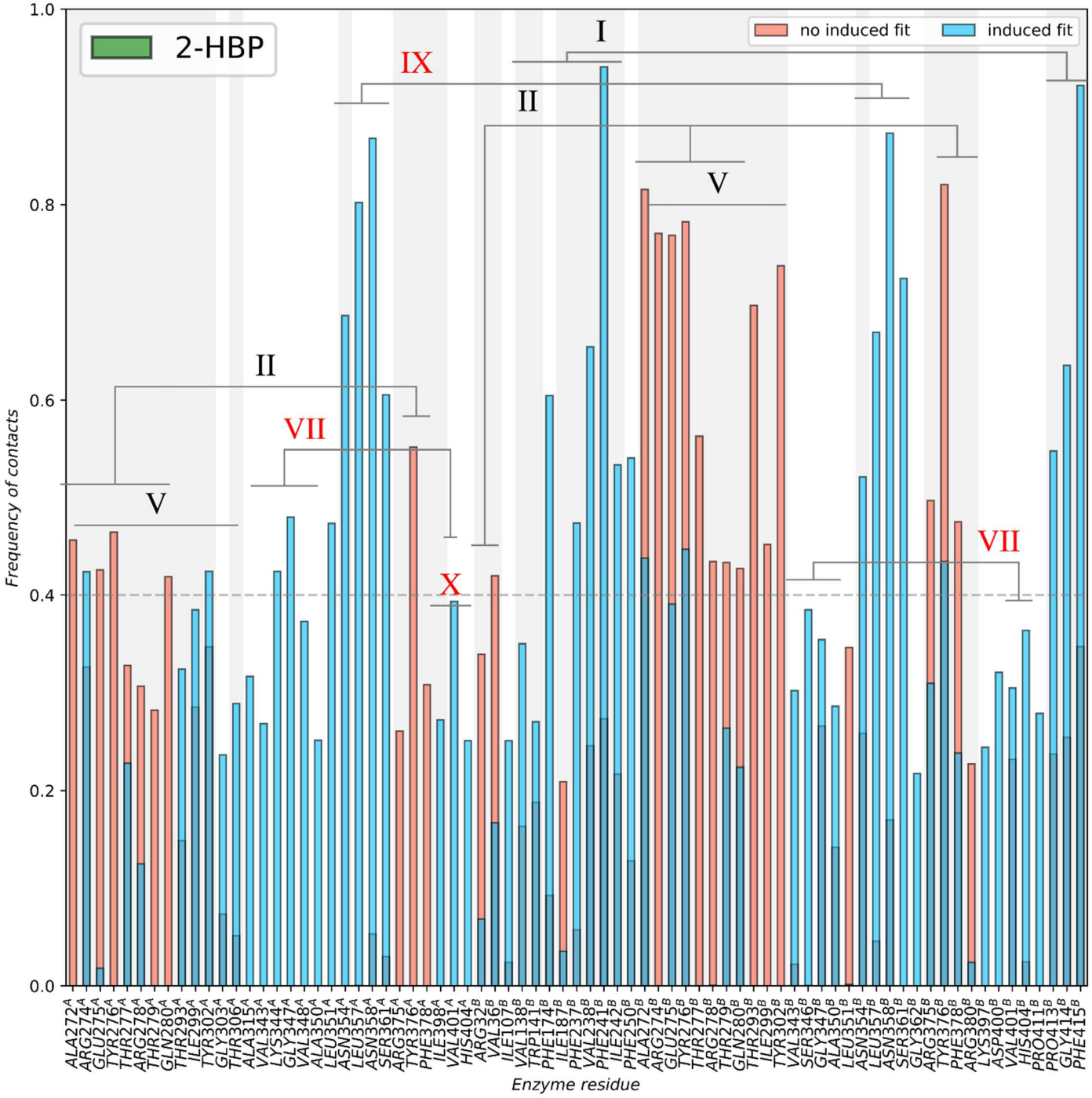

Figure S7. Summary bar plot with the frequency of contacts of 2-HBP molecules with DszC residues at a minimum distance of 3.5 Å, for the 200 ns molecular dynamics including five 2-HBP ligands, following the "no induced fit" and the "induced fit" protocols. Only residues that contact for more 20 % of the simulation time with 2-HBP are shown for simplicity. Residues composing the binding sites predicted from docking calculations are labelled with the roman number of the corresponding binding site.

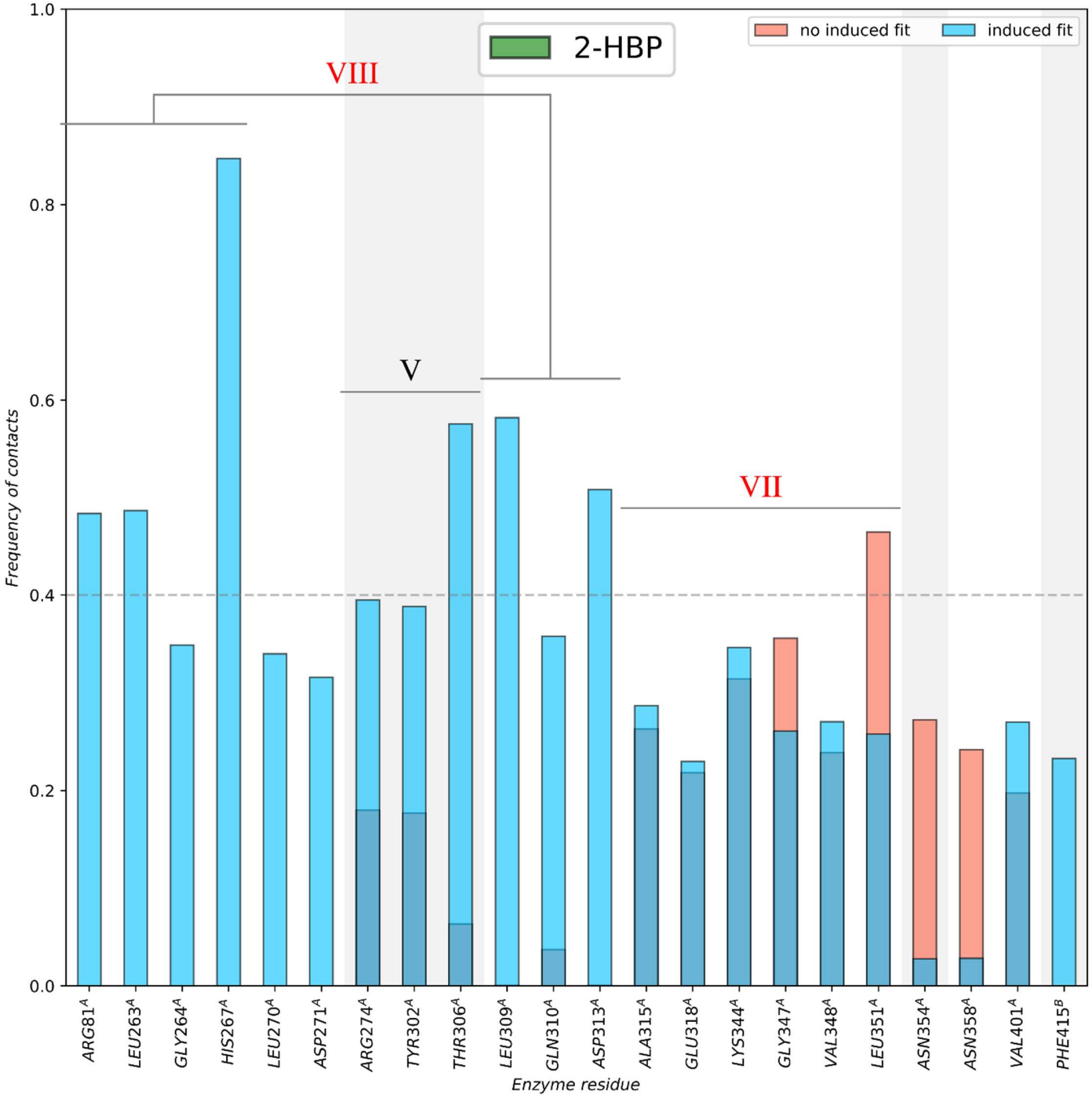

Figure S8. Summary bar plot with the frequency of contacts of 2-HBP molecules with DszC residues at a minimum distance of 3.5 Å, for the 200 ns molecular dynamics including two 2-HBP ligands, following the "no induced fit" and the "induced fit" protocols. Only residues that contact for more 20 % of the simulation time with 2-HBP are shown for simplicity. Residues composing the binding sites predicted from docking calculations are labelled with the roman number of the corresponding binding site.

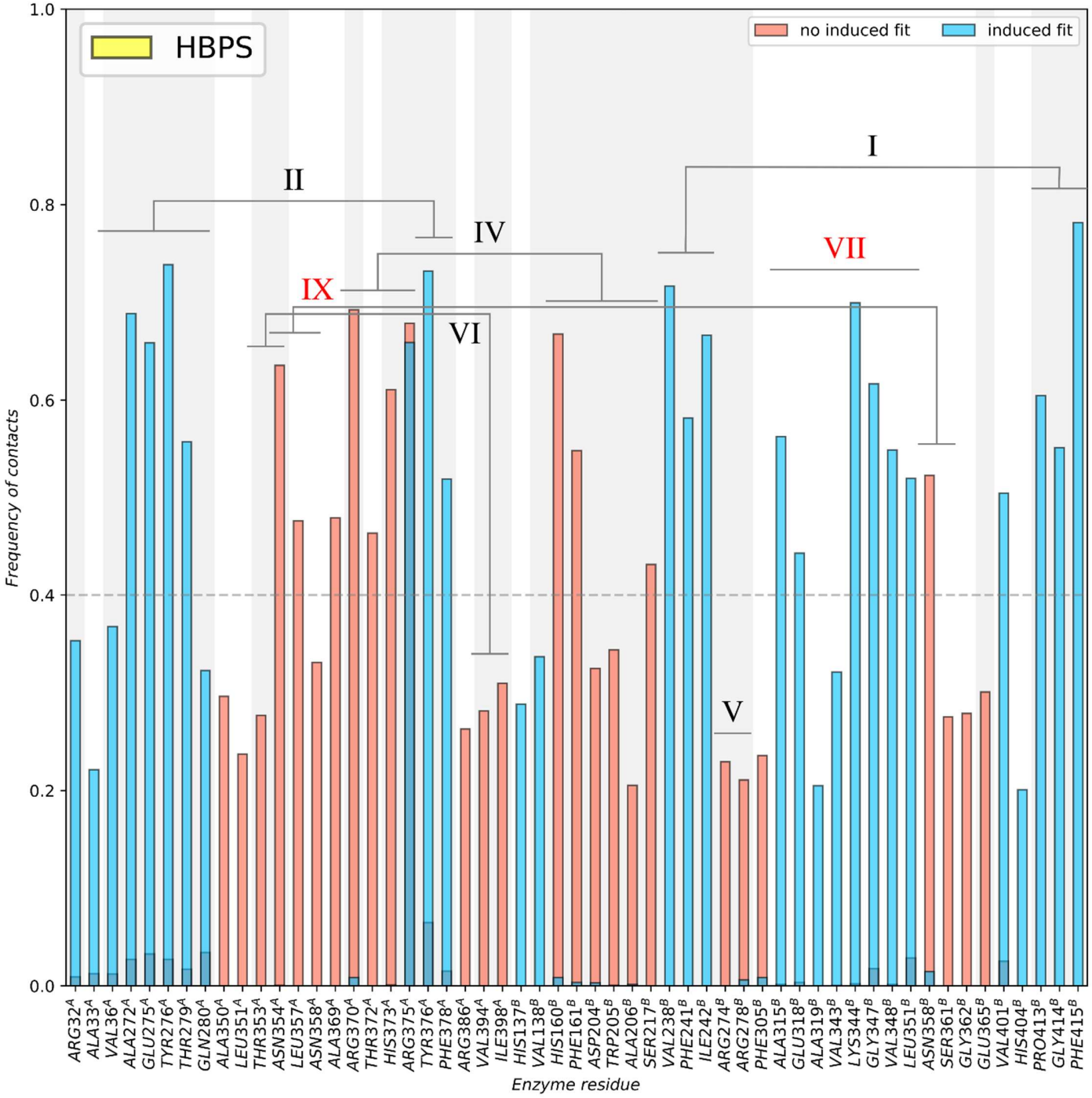

Figure S9. Summary bar plot with the frequency of contacts of 2-HBP molecules with DszC residues at a minimum distance of 3.5 Å, for the 200 ns molecular dynamics including four HBPS ligands, following the "no induced fit" and the "induced fit" protocols. Only residues that contact for more 20 % of the simulation time with HBPS are shown for simplicity. Residues composing the binding sites predicted from docking calculations are labelled with the roman number of the corresponding binding site.

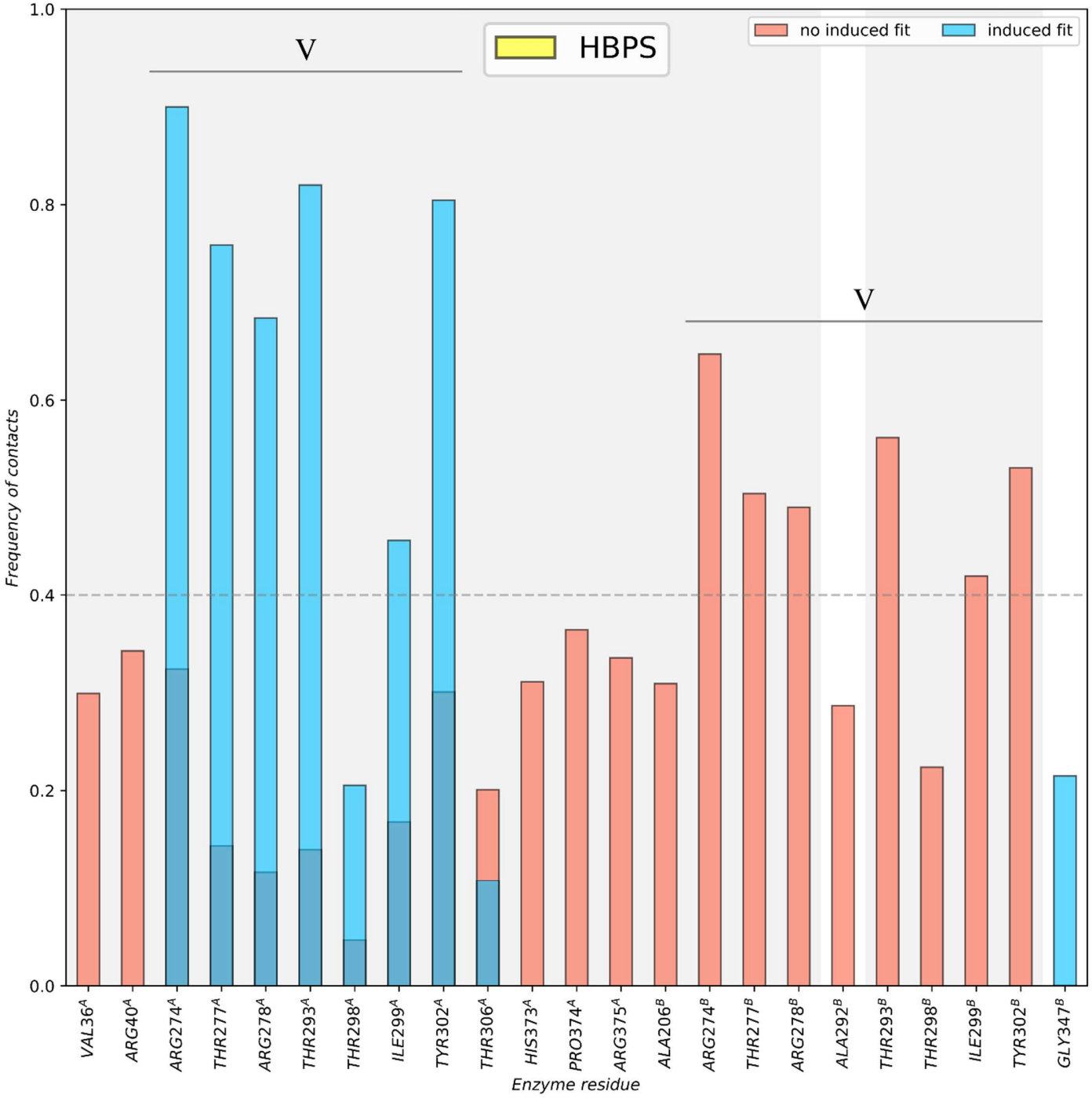

Figure S10. Summary bar plot with the frequency of contacts of 2-HBP molecules with DszC residues at a minimum distance of 3.5 Å, for the 200 ns molecular dynamics including two HBPS ligands, following the "no induced fit" and the "induced fit" protocols. Only residues that contact for more 20 % of the simulation time with HBPS are shown for simplicity. Residues composing the binding sites predicted from docking calculations are labelled with the roman number of the corresponding binding site.

Ranking and analysis of the DszC binding sites occupied by 2-HBP and HBPS

Table S1. Summary of the ranking of the binding sites identified for the eight 200 ns MD simulations ran. Binding sites occupied for over 60% of the simulation are marked with ✓; whether or not a corresponding representative binding mode was obtained upon clustering of the MD simulation a ✓ or ✕ were added in superscript. Entries colored in red correspond to binding sites occupied for less than 40% of the simulation.

BINDING SITE	5x 2-HBP		2x 2-HBP		4x HBPS		2x HBPS		TOTAL
	no induced	*induced*	*no induced*	*induced*	*no induced*	*induced*	*no induced*	*induced*	
I	✓✕	✓✓				✓✓			3
II	✓✓	✓✕				✓✓	✓✕		**4**
III		✓✓					✓✕		2
IV					✓✓		✓✕		2
V	✓✓	✓✕	✓✕	✓✕	✓✕	✓✕	✓✓	✓✓	**8**
VI					✓✕				1
VII		✓✓	✓✓	✓✕		✓✓			**4**
VIII				✓✕					1
IX		✓✕			✓✓				2

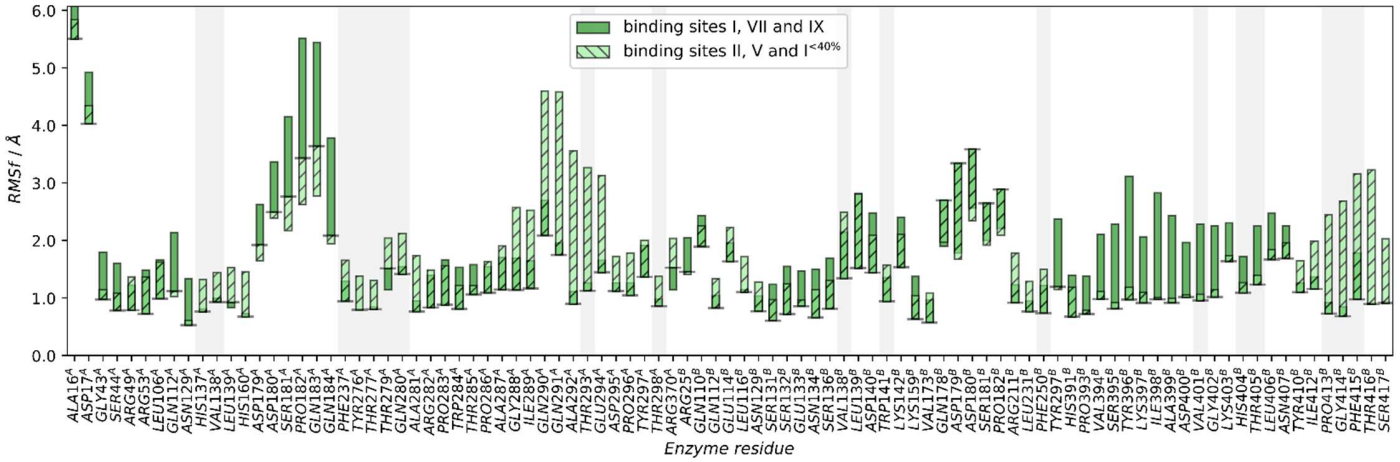

Figure S11. Bar plot of the RMSf registered for each of the two simulations where the best ranked binding sites (V, II, VII and I) were occupied by 2-HBP. The RMSf values from the simulation with no 2-HBP and HBPS were used as reference height for each bar, and only residues with a RMSf variation above 0.5 Å in at least one simulation were represented.

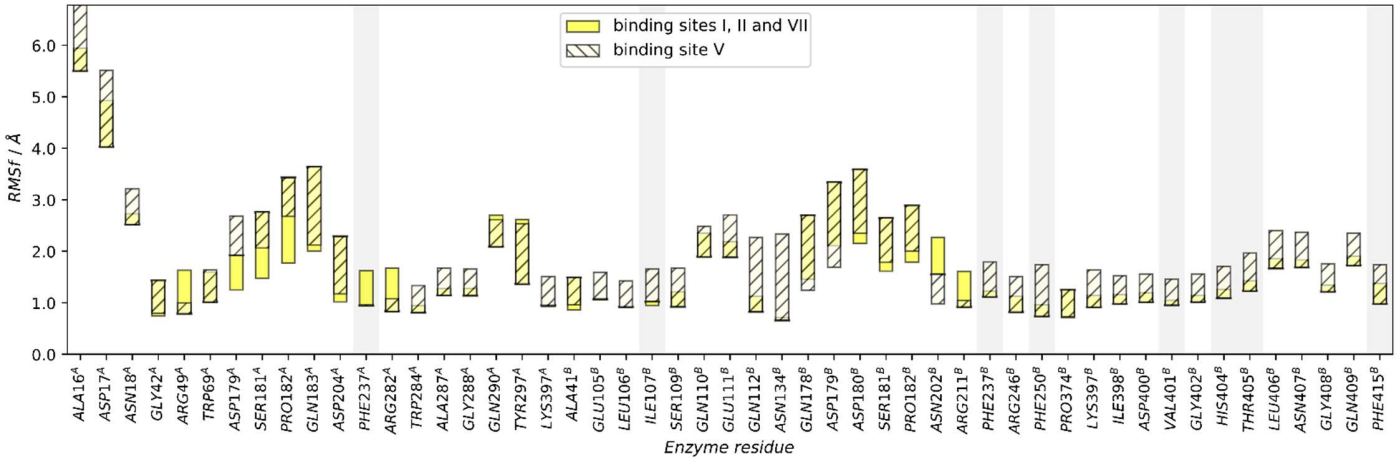

Figure S12. Bar plot of the RMSf registered for each of the two simulations where the best ranked binding sites (V, II, VII and I) were occupied by HBPS. The RMSf values from the simulation with no 2-HBP and HBPS were used as reference height for each bar, and only residues with a RMSf variation above 0.5 Å in at least one simulation were represented.